The Jahangirnagar Review: Part II: Social Science, Vol. 48, No. 1, 2024
ISSN 1682-7422 © Jahangirnagar University

Shoreline Change Analysis and Prediction of Sitakunda Coastline Using Satellite Imageries

Muhammad Khalilur Rahman[1]
Md. Shahedur Rashid[2]

Abstract: The term "shoreline" refers to the ever-evolving line denoting the border between water and land. This research, conducted in the Sitakunda area of Chattogram, accounted for the dynamic nature of the coast as a consequence of geomorphological and hydrological processes. The primary objective of the research is to analyze shoreline changes from 1990 to 2021. This study also tries to predict how shorelines will develop by the year 2034 using satellite imagery and the Digital Shoreline Analysis System (DSAS) in ArcMap software. Four multi-spectral satellite imageries have been used which are Landsat Thematic Map (TM) images (1990, 2000, 2011), and Landsat Operational Land Imager (OLI) images (2021) over the 31 years. The NDWI (Normalized Difference Water Index) technique was used to extract all of the previous shorelines. The shoreline change rates were calculated by using the End Point Rate (EPR) and Linear Regression Rate (LRR) method along the study area in four periods (1990-2000), (2000-2011), (2011-2021) and the global range of time (1990-2021). The highest erosion rate for the worldwide era is reported to be -16.72 m/year, while the maximum accretion rate is recorded to be 38.97 m/year. Erosion is most prominent at the shoreline's central section, whereas accretion is most prominent along its northern and southern sections. Erosion averaged -55.33 meters per year between 2000 and 2011, whereas accretion averaged 131.02 meters per year between 2011 and 2020. Erosion predominates from 2000–2021, while accretion predominates from 1990–2000 and 2011–2021. We were able to accurately predict the shoreline's position and length in 2034; it measured 42.78 kilometers length. The erosion and accretion area of the predicted shoreline is respectively 5.189 sq. km and 1.389 sq. km. The results identify the undisturbed and stable areas where future construction may proceed, as well as the most vulnerable areas that require immediate intervention. The DSAS approach is ideal for continuous monitoring of Sitakunda's shifting coastline.

Keywords: Landsat, DSAS, Remote Sensing and GIS, EPR, Bay of Bengal, LRR, NDWI

1. Introduction

Bangladesh's coastline zone is highly unstable and is changing over time according to the erosion and accretion process, as its territory is low-lying and a deltaic landform (Brammer, 2014). The coastal regions of Bangladesh are extremely susceptible to a wide variety of risks and calamities, including cyclones, storm surges, flooding, erosion, salinity, and more

1 Junior Consultant, Sustainable Forests and Livelihoods (SUFAL) Project, Forest Department, Email: khalilur.45@geography-juniv.edu.bd

2 Professor, Department of Geography and Environment, Jahangirnagar University, Savar Dhaka 1342, Email: m.s.rashid@gmail.com

(MoWR, 2006). As a result, it is crucial to recognize the dynamics of various coastal characteristics and their processes and to monitor the continual changes through precise detection and regular monitoring of shorelines (Kabir et al., 2020). On the other hand, it appears that more land was added to the Bangladeshi coast and offshore islands than was lost due to erosion between 1977 and 2010. Over the past 34 years, morphological changes in Bangladesh's coastal areas have resulted in a net gain of 139 square kilometers of land, which more than makes up for the expected submergence due to Relative Sea Level Rise (RSLR). Erosion is more prevalent on the eastern side, whereas accretion occurs on the southern and southwestern coasts (Uddin et al., 2013). Remote Sensing and Geographic Information System (GIS) approach can be easily used to identify the shoreline than other methods (Natesan et al., 2015). With the use of remote sensing, we are able to collect high-resolution, multispectral satellite images from all around the world and analyze them using ArcGIS, yielding outstanding findings for shoreline change (Aiello et al., 2013). Improvements in coastal geomorphological studies can be attributed to recent developments in remote sensing and geographical information system (GIS) techniques, such as the ability to semi-automatically determine shorelines, identify relative changes among coastal units, extract topographic and bathymetric information, and analyze them (Maiti and Bhattacharya, 2009).

This research applies remote sensing and GIS based DSAS tools to analyze and forecast future shoreline change using multi-spectral Landsat TM and OLI data collected from satellites. Additionally, the Sitakunda coastline change rate during the past three decades (1990-2021) will be estimated using End Point Rate (EPR) and Linear Regression Rate (LRR) models.

2. Study Area

Sitakunda shoreline in Chattogram District is the location under investigation; this area is typical of the northeastern Bay of Bengal. Its coordinates are 22°22' and 22°42' North, and 91°34' and 91°48' East (Figure 1). The 42.56 kilometers of coastline here are especially dynamics due to environmental and climatic changes. The forest covers 61.61 square kilometers of the 483.97 total square kilometers that make up Sitakunda Upazila. The Sandwip Channel in the Bay of Bengal is its western boundary. To the north is Mirsharai, to the south is Pahartali, to the east are Fatickchhari, Hathazari, and Panchlaish, and to the west is Mirsharai. A total of 298,528 people called Sitakunda home as of the 2001 census, with 163,561 men and 134,967 women (or a 121:100 gender ratio) living in 55,837 homes (with an average household size of 5.3) (Census, 2001).

Sitakunda is a 70 km long and 10 km wide geological structure located in western Chattogram and Chattogram Hill Tracts, bounded by the Feni River to the north, the Karnaphuli River to the south, the Halda River to the east, and the Sandwip Channel to the west. The Halda Valley and the Sandwip Channel are separated by the Sitakunda Range. One of Karnafuli's six tributaries, the 88-kilometer-long Halda runs from Khagrachari to the Bay of Bengal. Northernmost terminus of the western section of the Chattogram-Tripura Folded Belt is marked by Sandwip Channel. Sitakunda is located in a high-risk zone for cyclones and storm surges, having been hit by them on at least seven separate occasions between 1960 and 1997. Three of these cyclones—on May 29, November 12, and April 29—made landfall. The intra-deltaic coastline is frequently capable of creating tsunamis due to its proximity to the tectonic junction of the Indian and Burmese plates and the active Andaman-Nicobar fault system. Average yearly temperatures range from 32°F to 13°F, and 2,687 mm of rain falls each year. Between 1991 and 2001, the average annual wind speed in Sitakunda was 1.8 knots, or 2 mph (News Desk, 2009).

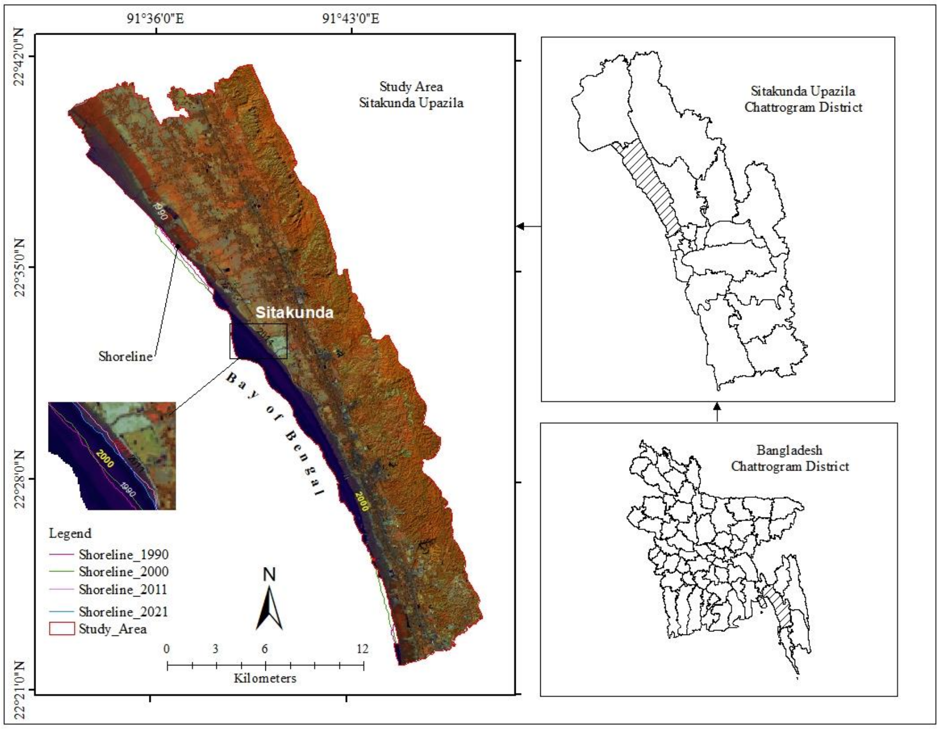

Figure 1: Study area map (Sitakunda Coastal Area)

3. Data

In this analysis, we used four different multi-spectral satellite images that span the 31 years from 1990 to 2021. Due to the lack of cloud-free imagery during the selected period, satellite images could not be obtained at regular intervals. Three Landsat TM images (1990, 2000, and 2011) and one Landsat OLI image (2021) were utilized for this analysis. The US Geological Survey's Earth Explorer website (*https://earthexplorer.usgs.gov*) is the source for these images as shown in Table 1.

Table 1: The utilization of images in this research studies to identify the shoreline changes.

Satellite	Sensor Type	Path/Row	Acquisition Date	Resolution	Cloud Cover	Source
Landsat 8	OLI	136/44,45	02/06/2021	30m	7	*Earthexplorer. usgs.gov*
Landsat 5	TM	136/44,45	02/14/2011	30m		
Landsat 5	TM	136/44,45	02/13/2000	30m		
Landsat 5	TM	136/44,45	02/17/1990	30m		

4. Methodology

Images are collected at level -1 processing, which is the products based on scenes and with the maximum processing level available for each scenario, using the World Geodetic System 1984 (WGS84) datum and the 38 degrees north latitude Universal Transverse Mercator (UTM) projection zone. Images are then double-checked for accuracy, and ArcGIS 10.6 is used to create a custom clipping mask of the research region.

4.1 Shoreline extraction

The location of the coastline is in a constant state of flux as a result of natural causes (Huang et al., 2019). The buffering method in the ArcGIS environment was used to establish the baseline. Many scientists agree that this line, known as the High-Water Line (HWL), should be used to demarcate the border between the beach and the water (Gokceoglu et al., 2015). Contrarily, the coastline was derived from these datasets (Table 1) by means of the Normalized Difference Water index (WI 2015) (Fisher et al., 2016). ArcGIS 10.6 was used to process a picture clip created in Erdas Imagine 2014, and the coastline was retrieved for four distinct time periods (1990, 2000, 2011, and 2021).

For Landsat 8,

$$NDWI = \frac{Band\ 3\ (Green) - Band\ 5(NIR)}{Band\ 3\ (Green) + Band\ 5\ (NIR)}$$

is the formula for calculating NDWI. (Fisher et al., 2016).

4.2 Shoreline Change Rates

The U.S. Geological Survey's Digital Shoreline Analysis System (DSAS) (Figure 2) is a plug-in for Esri's ArcGIS that computes shoreline change statistics using a time series of vector shoreline positions (between baseline and extracted shorelines) and features a beta model for forecasting shoreline position.(Rachel E., 2021)

Various DSAS algorithms and their uses in calculating shoreline statistics are covered in this lesson. Several methods exist for determining the rate of shoreline change: Net Shoreline Movement (NSM), Shoreline Change Envelope (SCE), End Point Rate (EPR), and Linear Regression Rate (LRR).

The NSM is measured in meters and is defined as the difference between the shorelines at the oldest and newest ages along each transect. Then, using the following formula, I determined the net shoreline movement.

$$\boldsymbol{Net\ Shoreline\ Movement = Distance\ Between\ Oldest\ and\ newest\ Shoreline}$$

To get the end point rate (EPR), we divide the distance of shoreline movement by the amount of time that has passed from the oldest and most recent shoreline. The determined end point rate (EPR) is used to determine the rate of change (Emily A. Himmelstoss, 2009).

$$End\ Point\ rate = \frac{Distance\ in\ meters}{Time\ bewteen\ Oldest\ and\ most\ recent\ Shoreline}$$

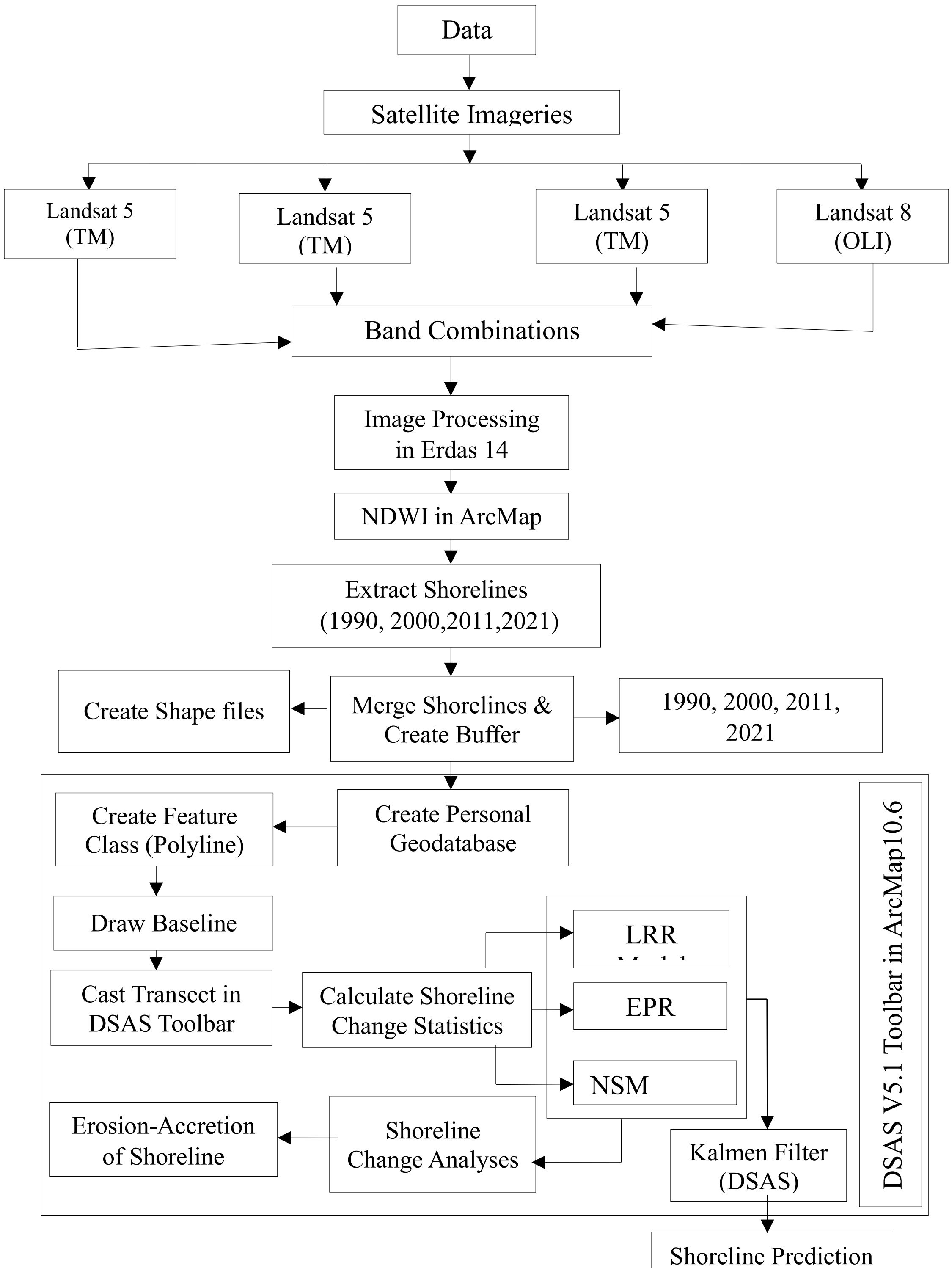

Figure 2: Methodology flowchart.

(Source: Modified after Najeeb S. Aladwani,2022 & DSAS Model from USGS)

4.3 Shoreline Prediction

Predictions of the shoreline can be made by The End Point Rate (EPR) model is one of many that have been tested and compared with historical data in order to make predictions about shorelines (Robert Dolan, 2011). The DSAS module includes beta shoreline forecasting algorithms that can extrapolate the shoreline's position 10 or 20 years into the future using data from the past (Rachel E., 2021) By integrating observed coastline locations with model-derived positions, the Kalman filter (Kalman, 1960) has been used in the shoreline forecasting computation (Long and Plant, 2012). Using the linear regression rate determined by DSAS and the Kalman filter method, we can predict the coastline location and change rate every 10 years and the associated positional uncertainty. After being processed, it yields a coastline that may be forecasted using historical coastline data.

5 Result and Discussion

5.1 Analysis Shoreline Change Rates

Eight hundred and twenty transect lines (Table 2) were drawn perpendicular to the baseline and intersected the four extracted shorelines at intervals of 50 m, completely encircling the coast and providing data on the rates of shoreline change over its whole length (about 42.56 km). The rates of change in the research region were determined using the EPR model for four-time intervals: (1990-2000), (2000-2011), (2011-2021), and the period (1990-2021) (Figure 3). Six stretches of shoreline, each with a different pattern of erosion and accretion as determined by an examination of historical data (Figure 3). There are three cross-sectional maps in (Figure 4) that provide illumination on these sections. Tables 3, 4, and 5 provide the descriptive statistics of shoreline change rates using the EPR model in DSAS for the global period (1990-2021), whereas Table 2 shows the statistics of shoreline change rates along the three periods.

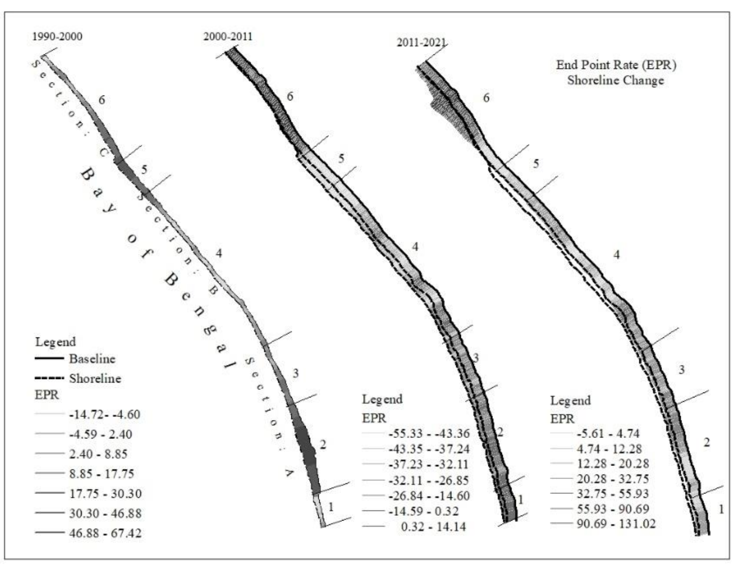

Figure 3: Shoreline rate changes across the three time periods using the EPR model 1990-2000,

2000-2011, 2011-2021.

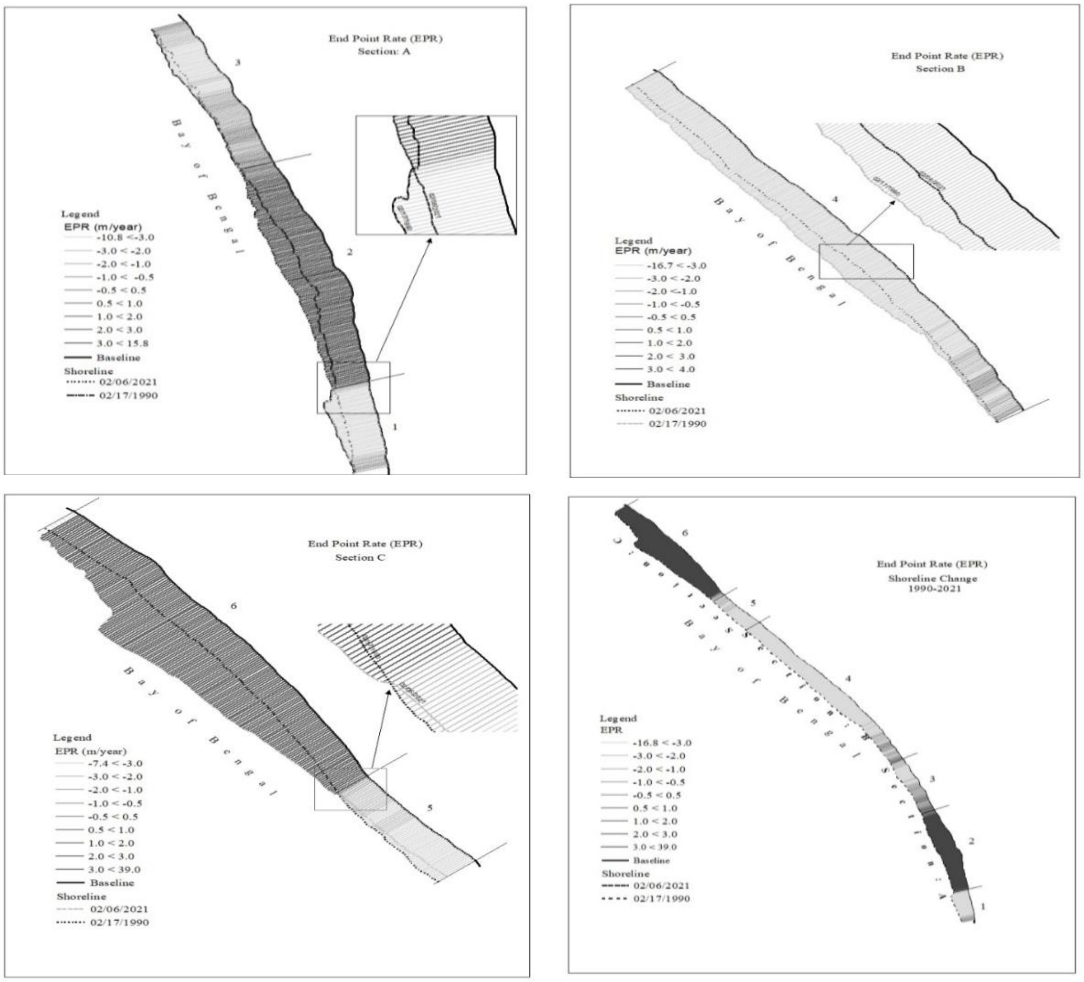

Figure 4: Shoreline segments displayed between Sections A, B, C, and whole shoreline change rates calculated using the EPR model for the years 1990-2021.

It has been calculated that, the average rate of 14.67 m/year, maximum erosion rate of -14.72 m/year, average of all erosional rates of -5.16 m/year maximum accretion rate of 67.42 m/year, and average of all accretional rates of 20.51 m/year in the period of 1990-2000.

In the period of 2000-2011, it has been found that, the average rate of -26.33 m/year, maximum erosion rate of -55.33 m/year, average of all erosional rates of -30.82 m/year maximum accretion rate of 14.14 m/year, and average of all accretional rates of 5.12 m/year.

The statistical calculated of the period of 2011-2021, the average rate of 21.69 m/year, maximum erosion rate of -5.6 m/year, average of all erosional rates of -2.15 m/year maximum accretion rate of 131.02 m/year, and average of all accretional rates of 23.07 m/year.

5.1.1. Area of Erosion

Segments 1, 3, and 5 comprise the largest portion of the eroding region, accounting for 59.88% (24.55 km) of the overall coastline length in the research. Erosion rates on the 419 transects analyzed varied from -16.72 m/year to 0 m/year (Figure 4) and as high as -53.3 m/year Table 4 and (Figures 3 and 7) for the duration of the period. Segments 1, 4, and 5 in the center of the study coastline noted the highest average erosion rates (-6.3 m/year), whereas segment 3 in the south experienced the lowest (-6.39 m/year). On the other hand, segment 6 in the north had the least amount of erosion overall (an average of -5.61 Table 5 throughout the whole time). Erosion rates ranged from -30.82 m/year in the second period (2000-2011) to -5.16 m/year in the first period (1990-2000) and -2.15 m/year in the third period (2011-2021) in the eroding regions (Table 3, 4, and 5) & (Figure 3).

Table 2: Rates of shoreline change calculated with DSAS's EPR model for the whole period 1990-2021

Section	Segment no.	Transects		Number of transect lines	EPR 1990-2021		
		From	To		Minimum	Maximum	Mean
Section A	1	1	52	52	-10.8	-0.82	-5.795
	2	53	192	140	0.65	15.75	8.392
	3	193	286	94	-6.39	1.56	-2.152
Section B	4	287	571	285	-16.62	-0.36	-8.109
Section C	5	572	632	61	-7.31	-0.39	-4.079
	6	633	820	190	1.37	38.96	20.875

Table 3: Rates of change in shorelines calculated with DSAS's EPR model from 1990 to 2000

Seg. No.	Transects		Number of transect lines	EPR 1990-2000		
	From	To		Minimum	Maximum	Mean
1	1	52	52	-14.72	17.49	-2.165
2	53	192	140	18	67.41	44.911
3	193	286	94	-2.15	22.17	11.862
4	287	571	285	-12.78	23.59	1.796
5	572	632	61	19.13	39.43	29.2
6	633	822	190	-10.88	38.9	13.019

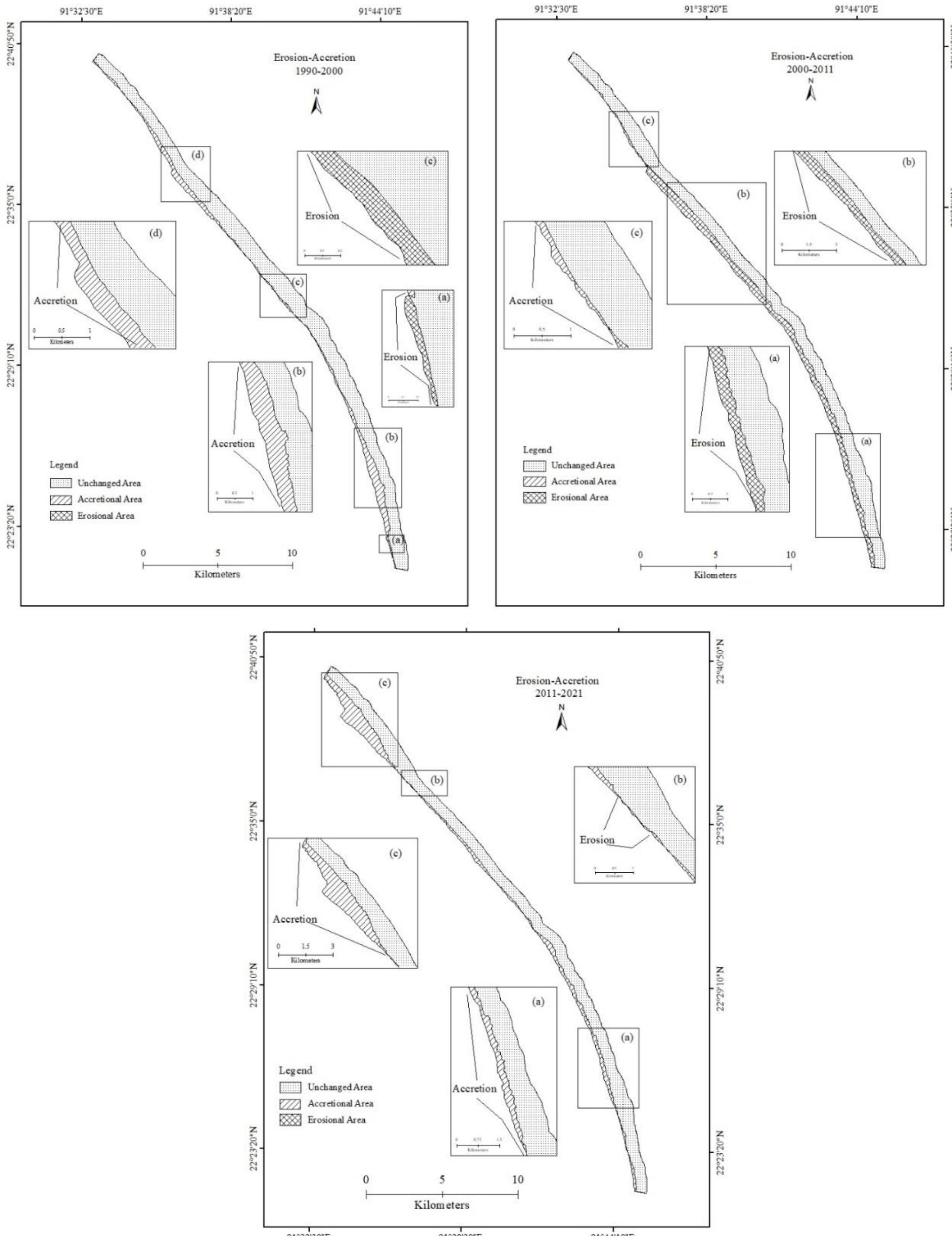

Figure 5: Erosion-accretion area and identified zone across the coastline of Sitakunda over 1990-2021.

Table 4: Rates of change in shorelines calculated with DSAS's EPR model from 2000-2011

Seg. No.	Transects		Number of transect lines	EPR 2000-2011		
	From	To		Minimum	Maximum	Mean
1	1	52	52	-31.45	-17.62	-24.86
2	53	192	140	-39.57	-17.4	-27.909
3	193	286	94	-42.38	-25.75	-32.562
4	287	571	285	-51.63	-20.17	-36.433
5	572	632	61	-53.33	-38.88	-45.986
6	633	822	190	-38.16	14.14	-1.261

Table 5: Rates of change in shorelines calculated with DSAS's EPR model from 2011-2021

Seg. No.	Transects		Number of transect lines	EPR 2011-2021		
	From	To		Minimum	Maximum	Mean
1	1	52	52	2.57	19.25	11.881
2	53	192	140	-3.46	33.22	12.737
3	193	286	94	6.63	27.1	17.725
4	287	571	285	-3.41	37.14	13.658
5	572	632	61	-1.55	12.61	6.692
6	633	822	190	-5.61	131.02	49.51

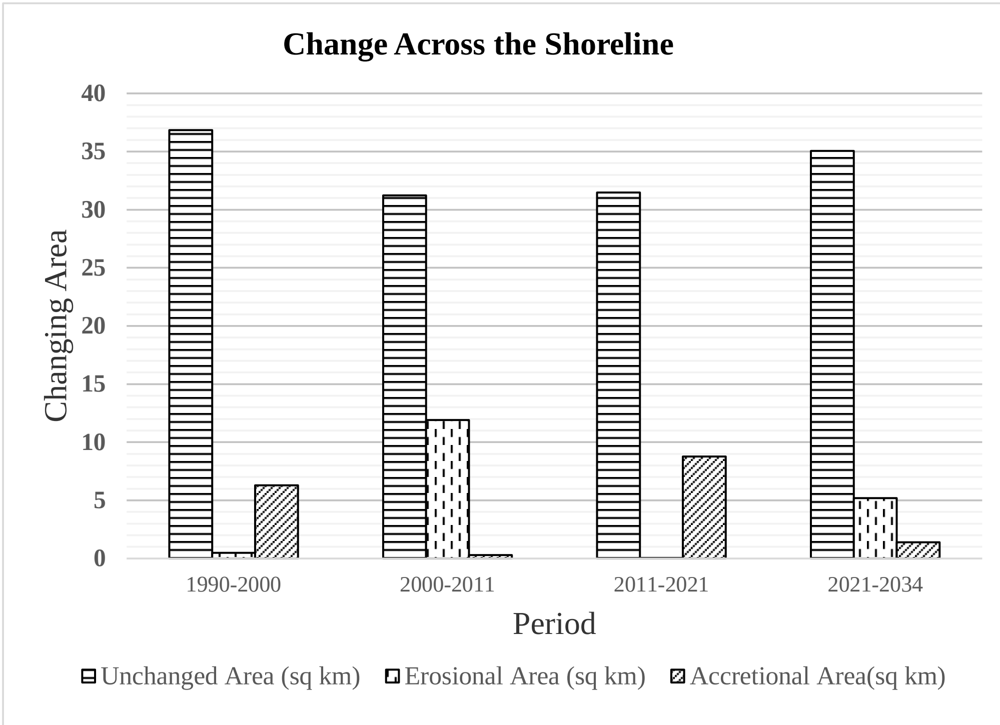

Figure 6: Changing area across the shoreline over different period (1990-2000), 2000-2011), (2011-2021), (2021-2034)

5.1.2. Area of Accretion

Segment numbers (2 and 6) in Figure 4 denote accretion regions. A total of 329 transects, covering 40.12% (18.01 km) of the coastline, were used to illustrate the accretion process in the studied region. The sand accumulated in two periods during the 1990-2000 and the 2000-2011 indicates a strong accretion mechanism along the shoreline, with the first period having an average accretion rate of 20.51 m/year and the third period having an average accretion rate of 23.07 m/year. However, accretion rates were at their lowest during the second period (2000-2011) (Figure 3, 5, 6 and 7), with an average of 5.12 m/year. For the whole time covered the study (1990-2021), the accretion rate is 15.11 m per year. Based on the total number of transects, the percentages of accretion area for the 1990-2000 (27.5%), the 2000-2011 (12.52%), and the 2011-2021 (94.54%) are documented in Table 6.

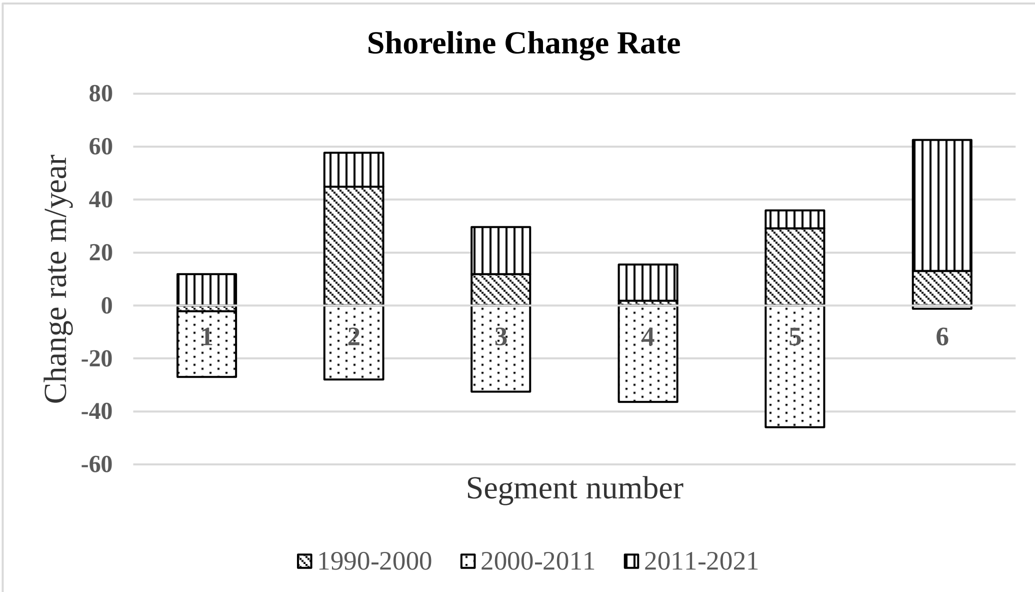

Figure 7: Every single period's range of shoreline change rates is plotted.

Table 6: Erosion and accretion rate based EPR method; included erosional and accretional are a percentage correspondent on transects number.

Period of Shoreline	Average erosional rates	No. of erosional transect ID	Transects (%)	Average accretional rates	No. of accretional transect ID	Transects (%)
1990-2000	-5.16	187	22.75	20.51	635	77.25
2000-2011	-30.82	720	87.48	5.12	103	12.52
2011-2021	-2.15	45	5.46	23.07	779	94.54

Figure 8: Erosion and accretion area over the 31 years, this diagram represents Section A

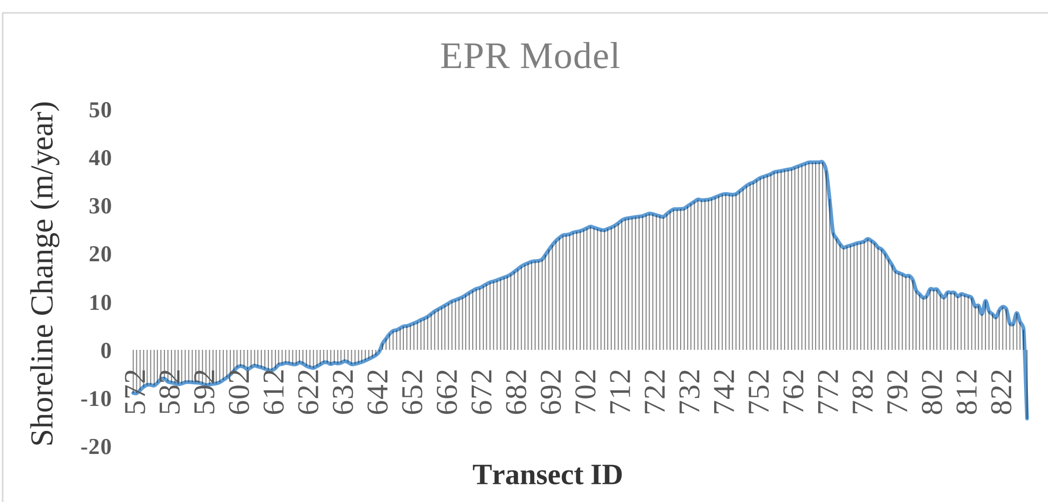

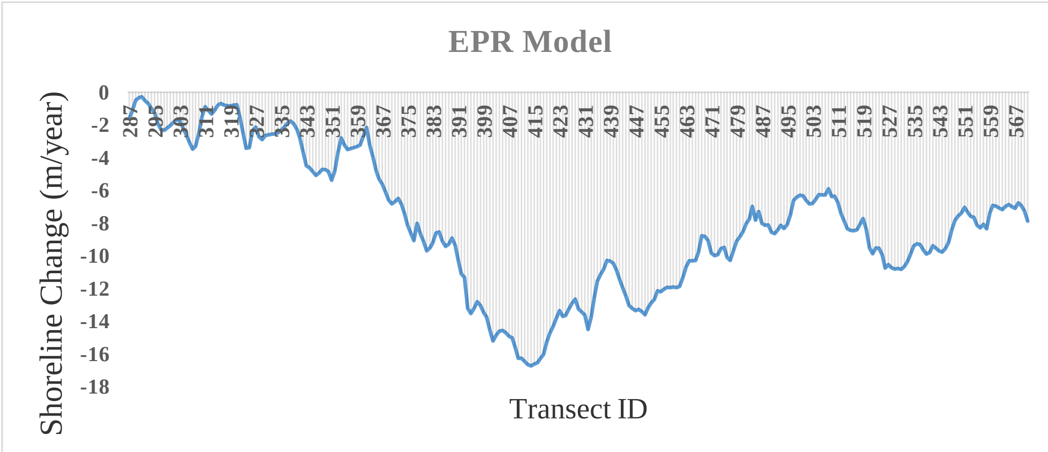

Figure 9: Erosion and accretion area over the 31 years, this diagram represents Section B

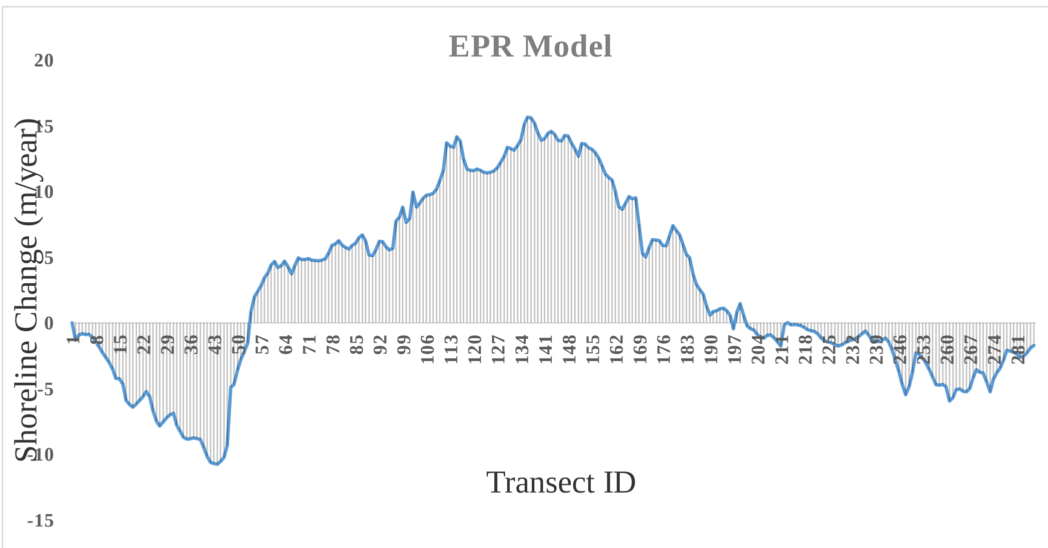

Figure 10: Erosion and accretion area over the 31 years, this diagram represents Section C

5.2 Shoreline Prediction

Based on its location in 2021, the EPR model predicted where the coastline will be in 2034. Past EPR rates calculated in 1990, 2000, 2011, and 2021 were used to make the forecast since they best capture the overall pattern of shoreline accretion and erosion. According to previous data, erosion will be most prominent throughout the shore's central region, while accretion will be particularly apparent towards the shore's extreme southern and northern reaches. (See Figure 11 and 12). In 2034, the length of the coastline is predicted to be 42.78 kilometers in Table 7.

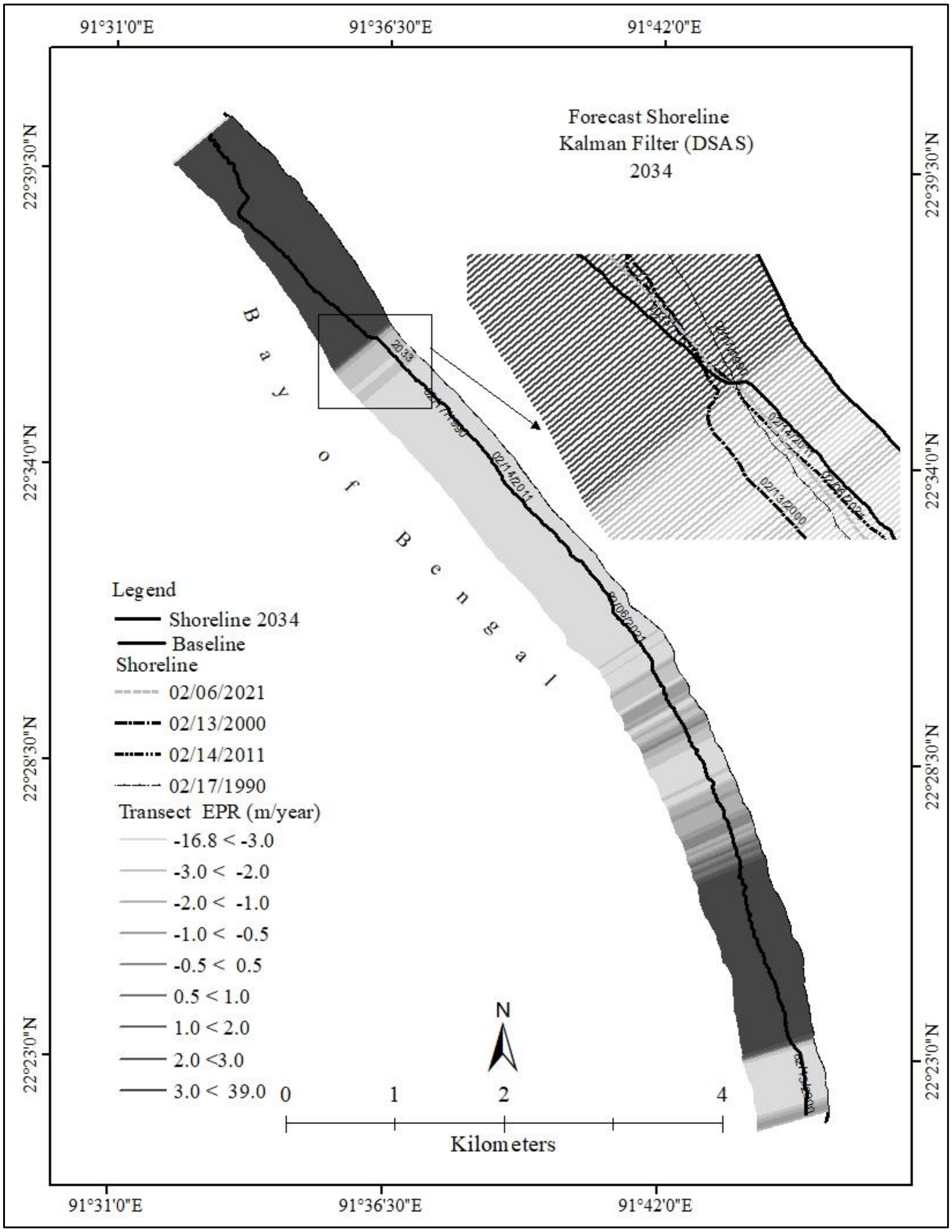

Figure 11: The shoreline forecasting calculation has done by using the Kalman filter (Kalman, 1960); it represents the predicted shoreline (2034)

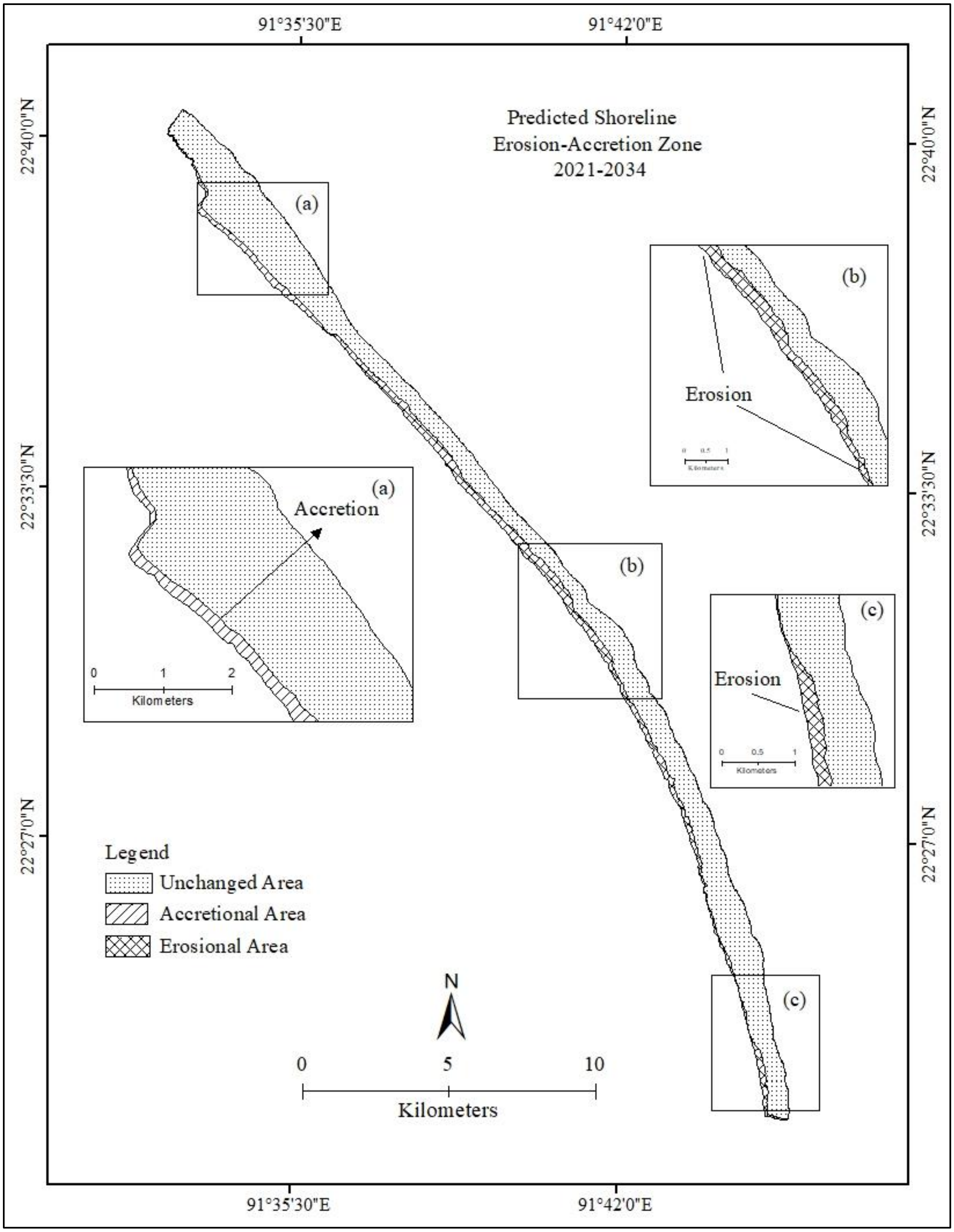

Figure 12: The erosion and accretional zone of pridicted shoreline.

In figure 11 and 12, The predicted shoreline created based on historical shoreline characteristics. The stable area has been found 35.055 sq. km. The erosion and accretion area is respectively 5.189 sq km and 1.389 sq. km. The central and sounthern part of this pridicted shoreline is dominated by erosion and the northern part is dominated by accretion. Since most of the area is undergoing erosion process, the loss should be reduced through proper planning and landuse of the shoreline.

6. Conclusion

By mapping out the areas of erosion and accretion along the Sitakunda coast, an investigation of shoreline changes over the last 31 years has helped researchers better comprehend shoreline migration. Using EPR models, we were able to extract the coastline's evolution across the time period of study and determine the rates of coastal erosion and accretion. The areas of the coast that are predicted to lose substantial ground to erosion will help direct area management toward providing immediate protection for future safe building. The results identify the undisturbed and stable areas where future construction may proceed, as well as the most vulnerable areas that require immediate intervention. The DSAS approach is ideal for continuous monitoring of Sitakunda's shifting coastline.

References

Aiello, A., Canora, F., Pasquariello, G., & Spilotro, G. (2013) 'Shoreline variations and coastal dynamics: A space–time data analysis of the Jonian littoral, Italy', *Estuarine, Coastal and Shelf Science*, 129, pp. 124–135. Available at: https://doi.org/10.1016/j.ecss.2013.06.012.

Aladwani, N.S. (2022) 'Shoreline change rate dynamics analysis and prediction of future positions using satellite imagery for the southern coast of Kuwait: A case study', *Oceanologia*, 64(3), pp. 417–432. Available at: https://doi.org/10.1016/j.oceano.2022.02.002.

Alizadeh, M. J., Alinejad-Tabrizi, T., Kavianpour, M. R., & Shamshirband, S. (2020) 'Projection of spatiotemporal variability of wave power in the Persian Gulf by the end of 21st century: GCM and CORDEX ensemble', *Journal of Cleaner Production*, 256, p. 120400. Available at: https://doi.org/10.1016/j.jclepro.2020.120400.

Atiquzzaman, M. and Kandasamy, J. (2016) 'Prediction of hydrological time-series using extreme learning machine', *Journal of Hydroinformatics*, 18(2), pp. 345–353. Available at: https://doi.org/10.2166/hydro.2015.020.

Brammer, H. (2014) 'Bangladesh's dynamic coastal regions and sea-level rise', *Climate Risk Management*, 1, pp. 51–62. Available at: https://doi.org/10.1016/j.crm.2013.10.001.

Chowdhury, P. and Sikder, Md.B. (2022) *Shoreline Dynamics of Reserved Region of Meghna Estuary and It Impacts on Lulc and Socio-Economic: A Case Study on Nijhum Dwip*. preprint. In Review. Available at: https://doi.org/10.21203/rs.3.rs-555094/v1.

Census,2001 "Bangladesh Population and Housing Census 2001 Zila Report – Chittagong"(bbs.gov.bd) Bangladesh Bureau of Statistics.

Deepika, B., Avinash, K. and Jayappa, K.S. (2014) 'Shoreline change rate estimation and its forecast: remote sensing, geographical information system and statistics-based approach', *International Journal of Environmental Science and Technology*, 11(2), pp. 395–416. Available at: https://doi.org/10.1007/s13762-013-0196-1.

Emily A. Himmelstoss, E.R.T. (2009) *The Digital Shoreline Analysis System (DSAS) Version 4.0 - An ArcGIS extension for calculating shoreline change*. 2008–1278. U.S. Geological Survey.

Esmail, M., Mahmod, W.E. and Fath, H. (2019) 'Assessment and prediction of shoreline change using multi-temporal satellite images and statistics: Case study of Damietta coast, Egypt', *Applied Ocean Research*, 82, pp. 274–282. Available at: https://doi.org/10.1016/j.apor.2018.11.009.

Fisher, A., Flood, N. and Danaher, T. (2016) 'Comparing Landsat water index methods for automated water classification in eastern Australia', *Remote Sensing of Environment*, 175, pp. 167–182. Available at: https://doi.org/10.1016/j.rse.2015.12.055.

Frihy, O.E. (2009) 'Morphodynamic implications for shoreline management of the western-Mediterranean sector of Egypt', *Environmental Geology*, 58(6), p. 1177. Available at: https://doi.org/10.1007/s00254-008-1595-3.

Gokceoglu, C., Nefeslioglu, H. A., Turer, D., Akgun, A., Ayas, Z., & Temimhan, M. (2014). 'Determination of coastal border line: an integrated approach for a part of Antalya coast (Turkey)', *Arabian Journal of Geosciences*, 8(2), pp. 1145–1154. Available at: https://doi.org/10.1007/s12517-014-1287-0.

Hakkou, M., Maanan, M., Belrhaba, T., El khalidi, K., El Ouai, D., & Benmohammadi, A. (2018). 'Multi-decadal assessment of shoreline changes using geospatial tools and automatic computation in Kenitra coast, Morocco', *Ocean & Coastal Management*, 163, pp. 232–239. Available at: https://doi.org/10.1016/j.ocecoaman.2018.07.003.

Huang, C., Wu, M., Sun, W., Bian, G., He, J., Deng, K., & Zhai, G. (2019). 'Improving the Definition and Algorithms of China's Coastline Considering the Diversity of Tidal Characteristics', *Marine Geodesy*, 42(4), pp. 382–405. Available at: https://doi.org/10.1080/01490419.2019.1610816.

Kabir, M. A., Salauddin, M., Hossain, K. T., Tanim, I. A., Saddam, M. M. H., & Ahmad, A. U. (2020) 'Assessing the shoreline dynamics of Hatiya Island of Meghna estuary in Bangladesh using multiband satellite imageries and hydro-meteorological data', *Regional Studies in Marine Science*, 35, p. 101167. Available at: https://doi.org/10.1016/j.rsma.2020.101167.

Kalman, R.E. (1960) 'A New Approach to Linear Filtering and Prediction Problems', *Journal of Basic Engineering*, 82(1), pp. 35–45. Available at: https://doi.org/10.1115/1.3662552.

Long, J.W. and Plant, N.G. (2012) 'Extended Kalman Filter framework for forecasting shoreline evolution: FORECASTING SHORELINE EVOLUTION', *Geophysical Research Letters*, 39(13), p. n/a-n/a. Available at: https://doi.org/10.1029/2012GL052180.

Maiti, S. and Bhattacharya, A.K. (2009) 'Shoreline change analysis and its application to prediction: A remote sensing and statistics based approach', *Marine Geology*, 257(1–4), pp. 11–23. Available at: https://doi.org/10.1016/j.margeo.2008.10.006.

MoWR (2006). Coastal Development Strategy. Water Resources Planning Organizations, Ministry of Water Resources, Government of the People's Republic of Bangladesh. pp. 1, 4-5.

Nandi, S., Ghosh, M., Kundu, A., Dutta, D., & Baksi, M. (2015) 'Shoreline shifting and its prediction using remote sensing and GIS techniques: a case study of Sagar Island, West Bengal (India)', *Journal of Coastal Conservation*, 20(1), pp. 61–80. Available at: https://doi.org/10.1007/s11852-015-0418-4.

Nassar, K., Fath, H., Mahmod, W. E., Masria, A., Nadaoka, K., & Negm, A. (2018) 'Automatic detection of shoreline change: case of North Sinai coast, Egypt', *Journal of Coastal Conservation*, 22(6), pp. 1057–1083. Available at: https://doi.org/10.1007/s11852-018-0613-1.

Natesan, U., Parthasarathy, A., Vishnunath, R., Kumar, G. E. J., & Ferrer, V. A. (2015) 'Monitoring Longterm Shoreline Changes along Tamil Nadu, India Using Geospatial Techniques', *Aquatic Procedia*, 4, pp. 325–332. Available at: https://doi.org/10.1016/j.aqpro.2015.02.044.

News Desk (23 January 2009), *AL supported candidates secure victory in 14 upazilas in Ctg*, Bangladesh Sangbad Sangstha, retrieved 28 January 2009

Rachel E. Henderson, E.A.H. (2021) *Digital Shoreline Analysis System (DSAS) Version 5.1 User Guide*. ISSN 2331-1258. U.S. Department of the Interior U.S. Geological Survey, p. 120. Available at: https://doi.org/10.3133/ ofr20211091.

Robert Dolan, M.S.F. (2011) 'A New Method for Predicting Shoreline Positions from Historical Data', *Coastal Education & Research Foundation*, Vol. 9,(No. 1 (Winter, 1993)), pp. 147–171.